References

1. B. BOVARNICK, "Interstitial Holes in the Ti–HCP Lattice", Watertown Arsenal WAL 401/122, o.o. Proj. No. T.B. (1952) 4.
2. D. R. MILLER, *Trans. AIME* **224** (1962) 275.
3. D. R. MILLER and K. M. BROWNE, "The Science Technology and Application of Titanium" (Pergamon Press, Oxford and New York, 1970) p. 401.
4. D. GUPTA and S. WENIG, *Acta Met.* **10** (1962) 292.
5. S. MISHRA and M. K. ASUNDI, "Titanium Science Technology", Vol. 2 (Plenum Press, New York, 1963) p. 883.
6. J. N. PRATT, W. J. BRATINA and B. CHALMERS, *Acta Met.* **2** (1954) 203.

Received 26 July and accepted 19 September 1977.

M. H. A. NAWAZ
Lehrstuhl für Werkstoffkunde und Werkstofftechnik, Agricolastr. 2, 3392 Clausthal-Zellerfeld, F.R.G.

Forming limit diagrams and damage in mild steel

Forming limit diagrams (FLD) have been empirically determined [1, 2] to describe the strain states of sheet metal. They are generally plotted in deformation space as ϵ_1 versus ϵ_2, these being the principal strains in the plane of the sheet. The FLDs at necking are of particular interest for determining the moment at which localized deformation appears. They have been studied for several metals and especially for mild steels.

Marciniak has proposed a theoretical analysis of the FLDs at necking [3]. In this analysis, the sheet is characterized by the rheological parameters n and R, the work-hardening exponent and anisotropy ratio respectively, and by an initial "geometrical" defect f_0.

In order to explain the whole FLD from uniaxial tension to biaxial stretching, it has been proposed to choose different parameters n [4] and R, depending on the strain path ρ ($\rho = \epsilon_2/\epsilon_1$); recent studies have confirmed this ρ dependence [5–7].

An alternative approach is to consider that the damage [8] increases continuously with deformation and in a different manner according to the strain path. It is then necessary to introduce an evolutive geometrical defect, f, whose amplitude depends upon the stress or strain tensor. This damage could be due to the existence of slip lines on the surface but this hypothesis is not realistic [9].

TABLE II Rheological parameters of the two SOLLAC steels [12].

Steel	n	R	Steel	n	R
Steel A	0.204	1.70	Steel B	0.208	1.83

The aim of this work is to show that the damage, which controls the necking, can result from the formation of voids at the matrix–particle interface. It has been known for a long time that this damage is responsible for ductile fracture, as proved by the examination of fracture surfaces [8]; but little work has been carried out on the growth of damage during deformation [10, 11] and the effect of different strain paths has never been studied.

The present work has been conducted on two SOLLAC steels of different compositions (Table I) but with similar rheological parameters (Table II). In spite of this rheological similarity their FLDs at necking, in the range where the strain ϵ_2 is positive, are quite different for biaxial stretching (Fig. 1) [12]. This study was carried out along the strain path where $\rho = 1$, which gives the maximum gap between the two FLDs.

TABLE I Chemical composition of the two SOLLAC steels [12].

Steel	Composition (wt % × 10)													
	C	Mn	P	S	N (total)	Al (metal)	Al (oxide)	Al (total)	Si	Cr	Cu	Ni	Mo	Ti
Steel A	51	325	15	13	7.9	42	5	47	58	–	–	–	–	–
Steel B	6	383	8	13	9.4	46	2	48	34	40	67	83	16	213

© 1978 Chapman and Hall Ltd. Printed in Great Britain.

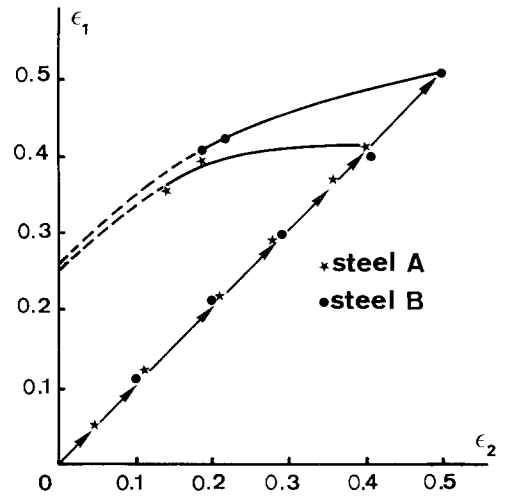

Figure 1 FLDs at necking of the two SOLLAC steels with the points where the different specimens were taken along the strain path $\rho = 1$ [12].

The damage was characterized by the measurement of the relative density change using Ratcliffe's method [13]. The accuracy of measurement ($> 10^{-5}$) necessitated the weighing of specimens of 100 mm^3 volume, all of which were taken from the top of stampings bulged by Jovignot's method.

Fig. 2 shows the relative density change of each steel as a function of the principal deformation ϵ_2. A threshold strain is found below which no density change is observed within the precision of the measurements. Such thresholds have also been observed in uniaxial tension [10, 11, 14]. Another result is that the steel A presents a relative density change greater than steel B, this difference increasing with strain. At points higher than the FLD at necking it becomes impossible to give precise values of the strains of a specimen because of the large gradient that develops in the sheets. However, the minimum strain ϵ_2 can be considered as constant above the FLD at necking [9], so that the relative density changes can be plotted.

It has been verified that these density changes were due to the formation of voids around inclusions (Fig. 3). In the present work, it is not possible to discuss the contribution of each type of inclusion to the damage, and thereby explain the differences in density change between steels A and B. Nevertheless, it seems certain that there is a great difference in the behaviour of the different types of inclusion.

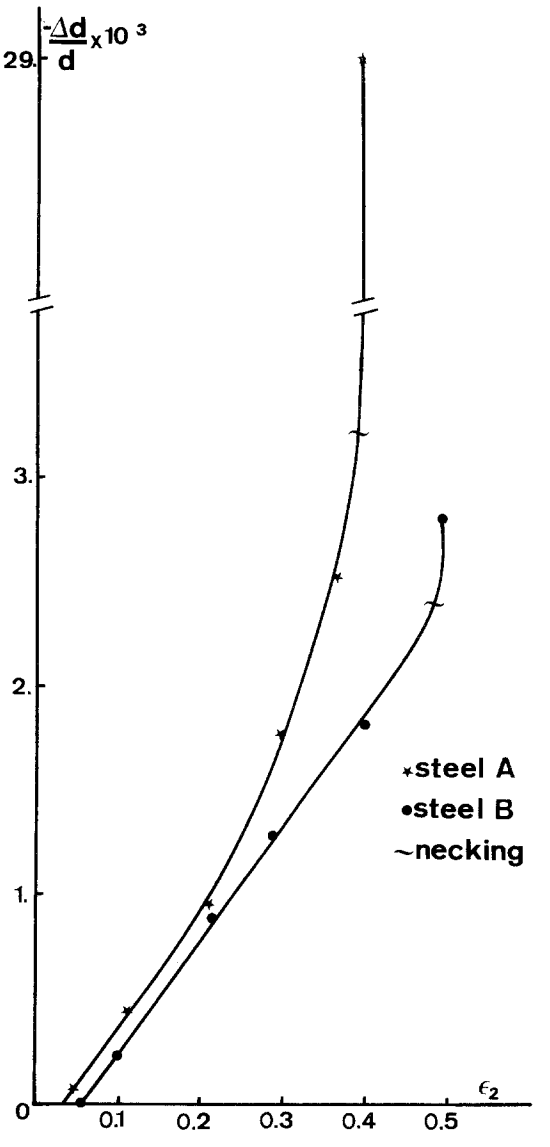

Figure 2 Relative density change along the strain path $\rho = 1$ for steels A and B. The level of the fracture point (upper one) is lower than the true value because of the strain gradient in the specimen.

Other studies have also shown the relative density changes of specimens deformed in uniaxial tension under different external hydrostatic pressures [15] or during extrusion [16]. They showed that the density changes are sensitive to the internal hydrostatic pressure, in agreement with theoretical analysis of void growth [17]. Our results are compatible with those obtained for steels under the same conditions of internal hydrostatic pressure [19, 15, 16]. Furthermore,

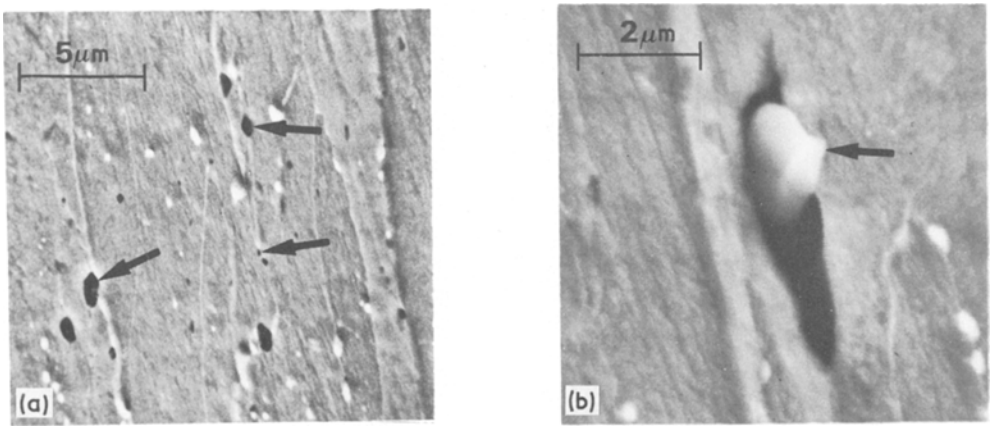

Figure 3 (a) SEM observation of voids on the surface of steel A deformed in biaxial stretching up to $\epsilon_1 = \epsilon_2 \simeq 0.4$. (b) SEM observation of void formed around an Al_2O_3 inclusion in steel A strained near necking.

for different strain paths $(0 < \rho < 1)$, it has been verified that the relative density changes are smaller when the lowering of internal pressure is smaller (i.e. when ρ tends to 0, Table III).

The density changes observed lead to relatively large geometric defects and therefore give values of the f index similar to those introduced in theoretical calculations. Thus this damage must be added to the initial geometrical defects due, in particular, to the surface roughness. The interest in the hypothesis of progressive damage is that it is not necessary to presume the existence of large initial defects f_0, which are incompatible with the quality of industrials sheets, for the explanation of FLDs.

This interpretation explains the relative positions of the FLDs of steels A and B. The lower FLD is for steel A which presents the greatest damage. Furthermore, the FLDs are closer when the strain paths are nearer plane stretching (i.e. $\rho = 0$) and similar relative density changes have been observed (Table III).

TABLE III Values of the relative density changes for the two SOLLAC steels for different strain paths and for strain states near the necking region.

Steel	ρ	ϵ_2	$-\Delta d/d \times 10^3$
Steel A	1.00	0.39	29
	0.46	0.18	1.73
	0.38	0.13	0.68
Steel B	1.00	0.49	2.8
	0.51	0.21	1.72
	0.47	0.19	0.46

This work shows that it is necessary to take into account the progressive growth of damage to explain the positions of the FLDs. As the origin of damage is the decohesion at particle–matrix interfaces, it is important to control the composition, shape and size of the inclusions because these greatly influence their contribution to the damage. Furthermore, the dependence of the damage on the strain path can help to explain the influence of complex strain paths on the position of the FLDs. After biaxial stretching the damage produced is greater than that produced during tension as a result of the greater lowering of pressure in the metal.

Acknowledgments

The authors express their thanks to the "Délégation à la Recherche Scientifique et Technique" for their financial support, to SOLLAC (M. Entringer, G. de Kainlis, D. Rault) for their collaboration and to A. Bilocq for technical assistance.

References

1. G. M. GOODWIN, *Metallurgia Italiana.* **60** (1968) 767.
2. S. P. KEELER, *Sheet Metal Industries* **42** (1965) 683.
3. Z. MARCINIAK, *Inst. J. Mech. Sci.* 9 (1967) 609.
4. A. K. GHOSH and W. A. BACKOFEN, *Met. Trans.* 4 (1973) 1113.
5. P. DELAYEN and P. PARNIERE, *Mem. Sci. Rev. Met.* 71 (1974) 67.
6. P. PARNIERE, *ibid* 74 (1977) 129.
7. F. RONDE-OUSTAU and B. BAUDELET, *Acta. Met.* **25** (1977) 1523.

8. G. HENRY, L. ROESH and J. PLATEAU, "Deformation plastique des métaux et alliages" (Masson Edition, France, 1968) p. 191.
9. M. ARZIN and W. A. BACKOFEN, *Met. Trans.* 1 (1970) 2857.
10. P. D. HOLMES, Ph.D. Thesis, University of Sheffield (1973).
11. J. D. ATKINSON, Ph.D. Thesis, University of Cambridge (1973).
12. M. ENTRINGER, G. DE KAINLIS, private communication (1977).
13. R. T. RATCLIFFE, *Brit. J. Appl. Phys.* 16 (1965) 1193.
14. J. LEMAITRE, J. P. CORDEBOIS, J. DUFAILLY, private communication.
15. D. W. WILSON, "Effect of Second Phase Particles on Mechanical Properties of Steel" (Iron and Steel Institute, 1971) p. 28.
16. H. C. ROGERS, "Metal Forming – Interaction between Theory and Practice" (Plenum Press, New York and London, 1971) p. 453.
17. J. R. RICE and D. M. TRACEY, *J. Mech. Phys. Solids.* 17 (1969) 201.

Received 26 July
and accepted 19 September 1977.

JEAN-MICHEL JALINIER
B. BAUDELET
Laboratoire de Physique et Technologie des Matériaux, Université de Metz, France
R. ARGEMI
Laboratoire de Physique du Solide, Ecole des Mines, Nancy, France

Improvement in the method for the impregnation of gypsum casts

Cast gypsum in the form of plaster of Paris casts and dies is particularly deficient in its mechanical properties [1–4]. A method reported to be effective in the enhancement of the properties of gypsum materials has been fully documented by Earnshaw [3, 4]. The method involved soaking the material in a liquid monomer to fill the void space and polymerizing *in situ* using thermal catalytic means. The reported new method [5] consists of an activated methyl methacrylate system that polymerizes in under 3 h and at ambient temperatures.

The specimens were prepared using an unmodified industrial plaster in various water–powder ratios and in various gang moulds (Table I). After casting the samples were removed and dried at 100° C for 24 h and were stored in a vacuum dessicator at room temperature prior to testing. The cast materials were immersed for approximately 1.5 h in a solution made up of methyl methacrylate (100 parts), lauroyl peroxide (4 parts) and N,N-dimethyl-p-toluidine (2 parts, wt/wt). When the temperature of the soak solution had risen to 60° C (about 90 min) the specimens were removed and allowed to stand at room temperatures for 30 min before testing.

Compressive, tensile and flexural strengths were determined using an Instron mechanical testing machine (Model TT(b)). Abrasion resistance was measured using a method similar to that reported by Mulhearn and Samuels [6]. Sample weight loss was recorded by abrading with a silicon carbide wheel under a 1 kg load for a period of 2 min. The results clearly demonstrate the enhancement in properties due to polymer impregnation and also the effects of varying the water–powder ratio (Table I).

TABLE I The effects of polymer impregnation on the properties of gypsum casts.

(a) Sample dimensions.

Test	Sample size
Compressive strength	25 mm o.d. × 45 mm.
Tensile strength	B.S. C.S.A. 25 mm × 25 mm.
Flexural strength	25 mm × 25 mm × 100 mm.
Abrasion resistance	25 mm × 25 mm × 25 mm.

(b) Compressive strength (N mm^{-2})

Water–powder ratio	Control	Impregnated	Strength factor
0.50	10.5	24.14	2.30
0.60	8.64	26.93	3.12
0.70	6.56	30.76	4.69
0.80	6.16	40.33	6.52

(c) Tensile strength (N mm^{-2})

Water–powder ratio	Control	Impregnated	Strength factor
0.50	1.10	5.76	5.23
0.60	0.99	6.40	6.47
0.70	0.76	6.72	8.84
0.80	0.60	6.16	10.26

© *1978 Chapman and Hall Ltd. Printed in Great Britain.*